Nanoscale

PAPER

View Article Online
View Journal

Cite this: DOI: 10.1039/c4nr01914h

Nanowire-based multifunctional antireflection coatings for solar cells†

Pritesh Hiralal,*[a] Chihtao Chien,[a] Niraj N. Lal,[b] Waranatha Abeygunasekara,[a,c] Abhishek Kumar,[a] Haider Butt,[d] Hang Zhou,[e] Husnu Emrah Unalan,[f] Jeremy J. Baumberg[b] and Gehan A. J. Amaratunga[a]

Received 9th April 2014,
Accepted 12th October 2014

DOI: 10.1039/c4nr01914h

www.rsc.org/nanoscale

Organic (P3HT/PCBM) solar cells are coated with ZnO nanowires as antireflection coatings and show up to 36% enhancement in efficiency. The improvement is ascribed to an effective refractive index which results in Fabry–Perot absorption bands which match the polymer band-gap. The effect is particularly pronounced at high light incidence angles. Simultaneously, the coating is used as a UV-barrier, demonstrating a 50% reduction in the rate of degradation of the polymers under accelerated lifetime testing. The coating also allows the surface of the solar cell to self-clean *via* two distinct routes. On one hand, photocatalytic degradation of organic material on ZnO is enhanced by the high surface area of the nanowires and quantified by dye degradation measurements. On the other, the surface of the nanowires can be functionalized to tune the water contact angle from superhydrophilic (16°) to superhydrophobic (152°), resulting in self-cleaning *via* the Lotus effect. The multifunctional ZnO nanowires are grown by a low cost, low temperature hydrothermal method, compatible with process limitations of organic solar cells.

Introduction

The last few years have seen a fourfold drop in the module price of solar cells.[1] Accompanied by high energy costs, photovoltaic (PV) energy has become an economically attractive candidate in many high insolation/high energy cost locations around the planet. Further reductions in cost and improvements in conversion efficiency are fundamental to further extend the range of locations in which photovoltaic energy is an economically sound option.

The current output of a photovoltaic cell depends principally on two factors; on the likelihood of an incident photon being absorbed, generating electron–hole pairs, and on the probability of the charge carriers being collected. The necessity of lowering costs is driving reduction in PV cell thickness, reducing the use of material as well as permitting the use of cheaper, low diffusion-length materials as the absorbing base.

Organic solar cells are a good example with rapidly improving efficiencies.[2] In a typical organic solar cell, light absorption creates strongly bound excitons that must be dissociated into free charges at a donor/acceptor interface. This need for exciton dissociation (diffusion length ~10 nm) complicates the design and fabrication of efficient organic solar cells, limiting the thickness of organic films to around 100 nm, which despite strong absorption, is insufficient to utilize most of the incoming light, particularly at longer wavelengths. The key solution is to enhance the optical path length by strongly trapping light within the cell. Various light trapping techniques have been proposed and explored. Electromagnetic field optimization by adjusting film thicknesses allows absorption to be increased.[3] Periodic gratings[4] can form oblique angle diffractions but are ineffective in preventing big reflection losses, and Bragg reflectors,[5] while having high reflectivity, can only double the optical path length. Photonic crystal back reflectors have been shown to increase optical path length by two orders of magnitude.[6] Surface plasmons in nanoscale metals have also been exploited to enhance absorption in PV cells.[7–9] Additionally, randomly or periodically nanostructured materials[10,11] have emerged as specific building blocks for constructing light-trapping assemblies.

Nanowire arrays show anti-reflective and light trapping properties; silicon NW arrays of a few microns in length have been

[a]Centre of Advanced Photonics and Electronics, Department of Engineering, University of Cambridge, 9 JJ Thomson Av., CB3 0FA Cambridge, UK. E-mail: pv237@cam.ac.uk; Fax: +44 (0)1223 748348; Tel: +44 (0)1223 748325
[b]NanoPhotonics Centre, Cavendish Laboratory, University of Cambridge, CB3 0HE Cambridge, UK
[c]Department of Electrical and Electronic Engineering, University of Peradeniya, Sri Lanka
[d]School of Mechanical Engineering, University of Birmingham, Birmingham B15 2TT, UK
[e]School of Electronic and Computer Engineering, Peking University, Shenzhen Graduate School, China
[f]Department of Metallurgical and Materials Engineering, Middle East Technical University, Ankara, Turkey
†Electronic supplementary information (ESI) available. See DOI: 10.1039/c4nr01914h

noted for their strong broadband optical absorption across multiple incident angles and their dark visual appearance.[12–14] This reduction in reflectance seems to be a common characteristic of nanowire arrays.[15–17]

Textured ZnO films by metalorganic chemical vapor deposition where considered as anti-reflection (AR) coatings early on.[18] ZnO has a wurtzite structure and due to the surface energetics of its crystal facets, easily grows as NWs.[19] The dimensions of these NWs can be easily controlled by the process parameters, and they can be produced at low temperatures and large scales,[20] making them attractive candidates for photovoltaic antireflection coatings.[21] ZnO NWs have already been coated onto Si solar cells,[22,23] demonstrating some improvement in efficiency.

In this work, we demonstrate ZnO NWs as antireflection coatings on organic photovoltaic cells for the first time. The ZnO NW coating brings additional benefits to photovoltaic cells, not previously studied in conjunction, namely UV protection and self-cleaning. The band-gap of ZnO (3.2 eV, ~380 nm) is just sufficient to absorb in the ultraviolet (UV) region. The organic components in OPVs are known to degrade in short times (few hours) under the combined presence of UV and O_2 or H_2O.[24]

We demonstrate the ZnO coating lowers the UV component reaching the organic layer and reduces the rate of degradation of the cell. ZnO is a photocatalytic semiconductor; the UV it absorbs in turn generates charge carriers which can be used to catalyse redox reactions in the presence of O_2 and water, permitting the breakdown of organic molecules on its surface.[25] This can be used as a self-cleaning mechanism for organic stains, addressing long term yield reduction issues from soiling.[26]

As grown ZnO is naturally superhydrophilic, however, adequate surface functionalisation can be used to lower surface energy, which combined with the high surface area of the NW coating yields a superhydrophobic structure.[27] in which the water–ZnO interface becomes energetically unfavourable and rain water droplets would simply roll off the surface, carrying dirt particles with them, known as the 'Lotus effect'.[28]

All three effects, namely AR, UV barrier and self-cleaning are demonstrated and characterized using the same ZnO NW coating over an organic solar cell. The AR properties are more pronounced when the incoming light is offset from normal incidence, which under a practical scenario forms the major part of a solar cells active life. The growth method used (hydrothermal) uses mild conditions and is compatible with the thermal tolerances of organic PV.

Experimental method

ZnO nanowire growth

Indium tin oxide (ITO) coated glass substrates (Delta technologies R_s = 10–12 Ohm per square) were cut and patterned by etching the undesired parts in hydrochloric acid (HCl 37%), and subsequently cleaned in an ultrasonic bath with acetone, and isopropyl alcohol successively for 10 min, then dried in nitrogen. ZnO nanowires were grown on the back (glass) side hydrothermally according to the method developed by Greene *et al.*[29] A 10 mM solution of zinc acetate dihydrate (98%, Aldrich) was prepared in 1-propanol (spectroscopic grade). The solution was then spin-coated on the glass substrate at 2000 rpm for 30 s. The substrates were then annealed at 100 °C for 1 min to form ZnO nanocrystals. Spin-coating and annealing processes were repeated 4 times. After uniformly coating the substrate with ZnO seeds, vertical nanowires were grown by dipping the substrate in a mixture of equimolar 25 mM hexamethylenetetramine(HMTA) and zinc nitrate hexahydrate ($Zn(NO_3)_2{\cdot}6H_2O$, Aldrich) solution at 90 °C for 2 hours. The morphology and size of the ZnO nanowires was investigated by field emission scanning electron microscopy (FESEM) (JEOL 6340F, operated at 5 kV), (Fig. 1). The crystallinity of the ZnO nanowires (not shown) was confirmed by high resolution transmission electron microscopy (HRTEM) (JEOL 3011 operated at 300 kV) and X-ray diffraction (XRD) with Philips PW1730 diffractometer with Cu Kα radiation.

After 2 hours of growth time, the NWs exhibit a diameter of 30–60 nm and a length of ~450 nm. XRD spectra (not shown[20]) show that ZnO nanowires grow preferentially along the [0001] direction. The final result is a glass substrate coated

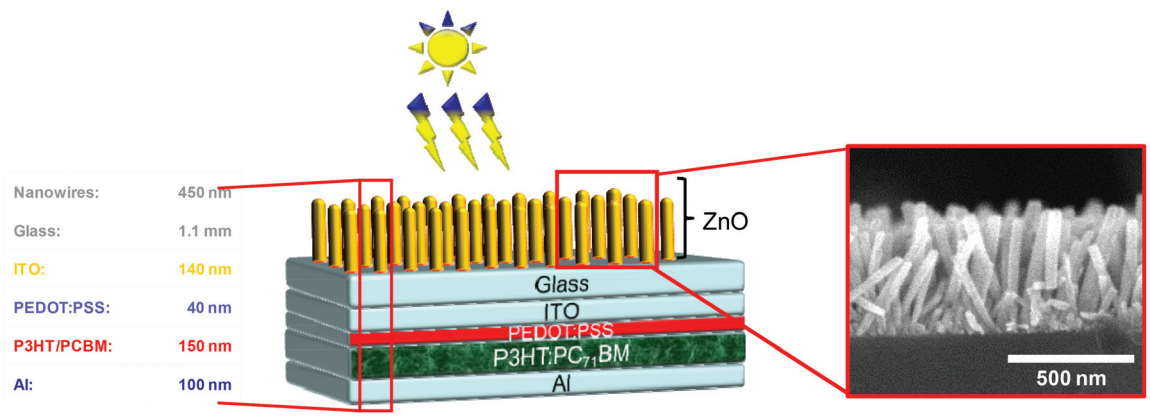

Fig. 1 Structure of the fabricated photovoltaic device (not to scale). The inset shows a scanning electron microscope image of the ZnO NWs.

with patterned ITO on one side and vertically aligned ZnO NWs on the other.

Organic photovoltaic device fabrication

The active material of the organic photovoltaic devices was prepared by dissolving [6,6]-phenyl-C61-butyric acid methyl ester (PCBM, Solenne) in dichlorobenzene and then blending regioregular poly(3-hexylthiophene-2,5-diyl) (P3HT, Sepiloid P200, Rieke Metals) with an average molecular weight, M_w = 20–30 K, without further purification. The resulting solution of 64 mg ml^{-1} concentration at 1 : 1 ratio was left stirring overnight at 45 °C.

Poly(3,4-ethylenedioxythiophene) poly(styrenesulfonate), (PEDOT–PSS, Baytron P 4083) was deposited by spin coating at 5000 rpm onto the pre-patterned ITO substrate and then dried at 135 °C for 15 min, resulting in a 40 nm film. Subsequently, the devices where moved into a N_2 glovebox for deposition of the photoactive layer. The P3HT–PCBM solution was deposited by spin casting at 1300 rpm. 100 nm thick Al electrodes were deposited *via* thermal evaporation (pressure ~3×10^{-6} Torr), resulting in active device areas of 8 mm^2. After evaporation, the devices were further annealed at 150 °C for 5 minutes. The structure of the resulting device is shown in Fig. 1. Typically, 8 devices were fabricated per substrate and each individual substrate had 4 of the 8 devices covered with ZnO NWs, in order to minimise interdevice variations.

The solar cells were characterized immediately after fabrication in ambient air environment at room temperature. External quantum efficiency (EQE) spectra were measured using a 100 W tungsten halogen lamp, dispersed through a monochromator. A Keithley 237 source measure unit was used to measure the short circuit current as a function of wavelength. The incident light intensity was continuously monitored during measurement by a reference photodiode calibrated by placing a Hamamatsu S8746-01 calibrated photodiode at the sample position. The current–voltage (*I–V*) characteristics of the devices were measured using a computer controlled HP 4140 source meter. An AM 1.5 solar simulator (Oriel 67005 with AM1.5 filter) at 100 mW cm^{-1} was used as the illumination source.

Results and discussion

Antireflection

Angularly resolved reflectivity measurements (Fig. 2(a) and (b)) were taken with a supercontinuum white-light laser obtained *via* the non-linear dispersion of a passively mode locked 1064 microchip laser (JDS Uniphase) focused through a holey fibre (Blaze Photonics). The beam has mixed polarization with a wavelength range of 500–1500 nm and angle range of 0–60 degrees. Results displayed are the log of reflectance, normalised to flat silver. The power of the beam is <1 mW and the collection area is approximately 200 μm in diameter.

NWs act as an anti-reflection coating by providing an effective refractive index between air and ITO glass. Angularly resolved reflectance of the NW coated sample shows distinct Fabry–Perot absorption bands (red-white curves), which undergo a typical blue shift (increase in frequency) with increase in incidence angle. The absorption enhancement occurs at energies which are typical of the band-gap of polymers used for OPVs (~1.9 eV).

Finite element method (FEM) simulations were carried out to simulate the wave propagation across a single ZnO nanowire and to understand absorption bands. To demonstrate that the ZnO NWs act as cavity towards the incident light (producing the blue shifting absorption bands) and for the purpose of simplification a single NW with a radius of 40 nm and height 0.45 μm (average value) was simulated in a three dimensional geometry. Non-periodic/scattering boundary conditions were used around the NW. The NW was illuminated with a plane wave light source in the range of around 478 nm to 1500 nm (~0.83 eV to 2.6 eV). The light was polarized parallel (TM mode) to the NW. Simulations were performed for incidence angles of 0, 30 and 60 degrees with the vertical. Fig. 2(c) shows the transmission spectra simulated for the three incident angles. The spectrum for zero degrees shows only two weak resonant cavity modes for the NW. However, at 30 and 60 degrees a number of cavity modes were coupled into the NWs. For the incident angle of 30 degrees resonant modes were observed at around 1.40,1.90 and 2.45 eV. For the 60 degrees incident light resonant modes were observed at around 1.8 and 2.5 eV. The resonant peaks were observed to blue shift with the increase in incident angle. These results demonstrate the cavity resonance of the ZnO nanowire and explain the absorption bands in the measured spectra. However, in the experiments an average cavity effect of many NWs resonating simultaneously is observed. As not all the NWs are oriented normally, due to which they resonate at a slightly different wavelengths for a certain incidence angle of light. Both the effects result in the broadening of the experimentally measured absorption bands.

Distribution in NW length results in an overall graded density and effective refractive from the glass towards the air interface. Fig. 2d shows the results from a simulation in which a periodic condition is applied. ZnO nanowires were represented as a periodic array nanowires of square shaped cross section. The simulation was done for nanowires of uniform cross section and also for tapering cross sections to take the overall graded nature into account. A good correlation is observed with experimental data (Fig. 2a).

J–V characteristics of OPV cells with and without ZnO coating are shown in Fig. 3(a) for different angles of incidence of the light. The light source intensity and position is maintained constant throughout the experiments, and the incidence angle was changed by tilting the solar cells. In effect, this resulted in a lower intensity of light reaching the cells upon tilting. A ~17% enhancement in efficiency is observed at normal incidence for the NW samples. The ZnO coated samples consistently had a larger open circuit voltage, and typically a larger short circuit current than the plain, reference samples (Fig. 3(b) and (c)). The light intensity dependence of V_{oc} has been previously explained,[31] and together with the increase in J_{sc} with the coating, suggests that the reduced

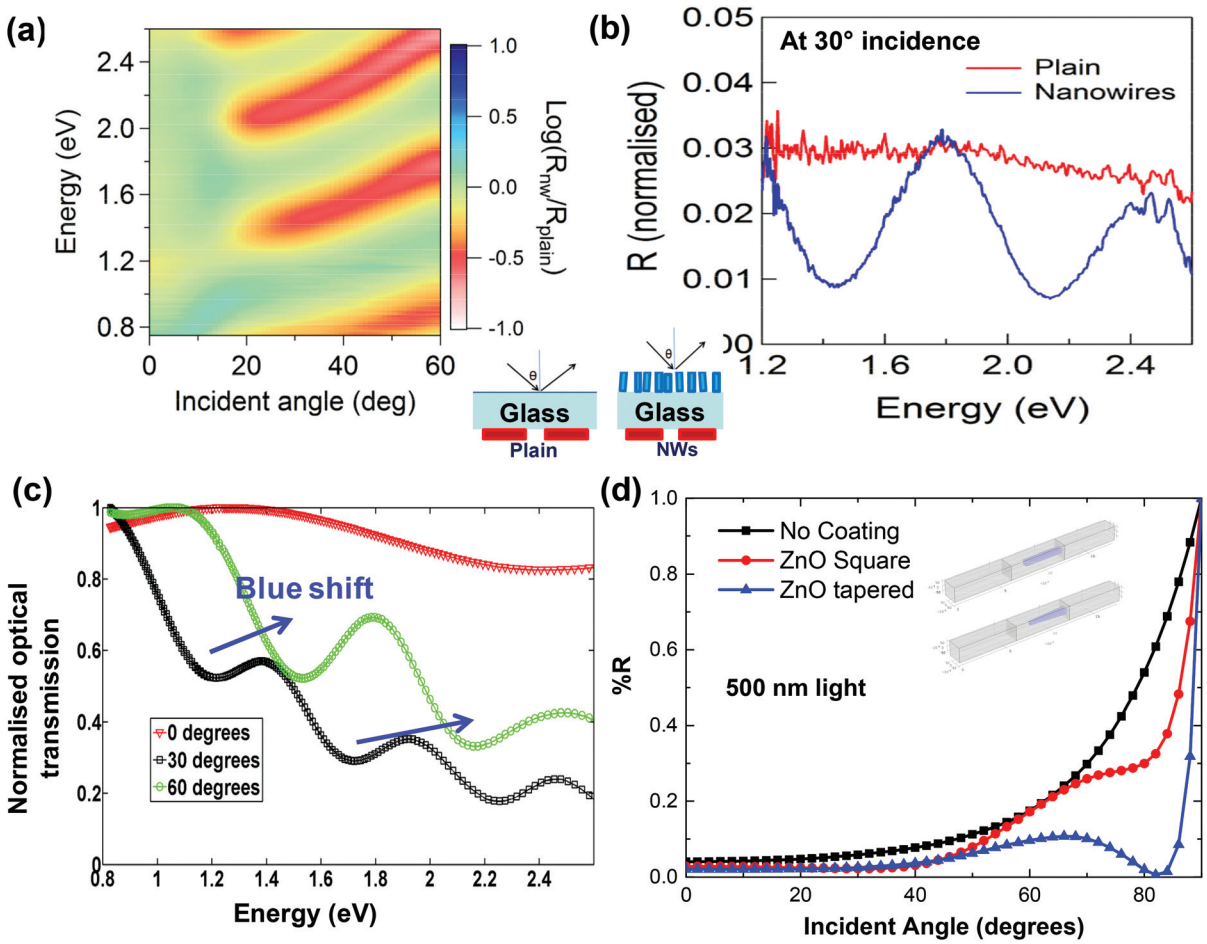

Fig. 2 (a) The angularly resolved reflectance spectra of plain and NW devices, normalised to silver. The relative angularly resolved reflectance spectra, highlighting the differences between the plain and NW devices ($\log(R_{nw}/R_{plain})$) is shown. Blue shows high reflectance and red-white shows low reflectance. (b) Normalised reflectance at 30 degrees. (c) Simulated single NW optical transmission spectra across the NW resulting from the cavity effect. (d) Simulated reflection of 500 nm light from the array of ZnO NWs.

reflection is correlated with more light being coupled into the active material. Given the common variation of performance in this kind of samples, the worst and best case scenarios are shown for the coated samples.

Fig. 3(d) summarizes the overall efficiency of the cells with respect to light incidence angle. The power input in the efficiency calculations is corrected to that reaching the cells as a result of the tilt. The strongest advantage of AR coated samples can be observed at 60° incidence (36% improvement), where the plain sample experiences a significant decrease in efficiency whilst the coated ones improve. This result correlates well with the reflectance spectra in Fig. 2(b), where both Fabry–Perot absorption bands occur above ~1.8 eV, matching the polymers band-gap.

The variation in the performance of the ZnO coated cells was larger than that of the plain cells. This is ascribed to the quality and morphology of the as-grown ZnO films. The average and standard deviation of the samples measured is shown in Fig. 3(e).

Fig. 3(f) shows typical EQE spectra of the devices. The baseline device shows a maximum EQE of 60% at 485 nm and broad shoulder at 600 nm which is consistent with the literature.[30] After incorporating ZnO nanowires, the EQE of the devices increased in the range of 480 nm to 610 nm. The EQE of the ZnO coated devices shows a sharp fall at wavelength less than 400 nm, which matches well with the UV-absorption of the ZnO nanowires.

The improved coupling of light into the active layer has previously been reported by using optical spacers, typically made of a TiO_2 layer placed between the active layer and the Al back contact.[32] However, there is one fundamental problem with TiO_2 based optical spacers which has not been tackled in the literature. TiO_2 is photocatalytic, and under the presence of UV results in the breakdown of organic molecules. In practical applications, this may pose a serious limitation for the lifetime of the device. The ZnO NW solution, in which the coating lies outside the device, may be a more practical solution to the problem.

Cell lifetime – UV-protection

The simultaneous presence of UV light and O_2/H_2O degrades semiconducting polymers.[24] The transmission spectrum of

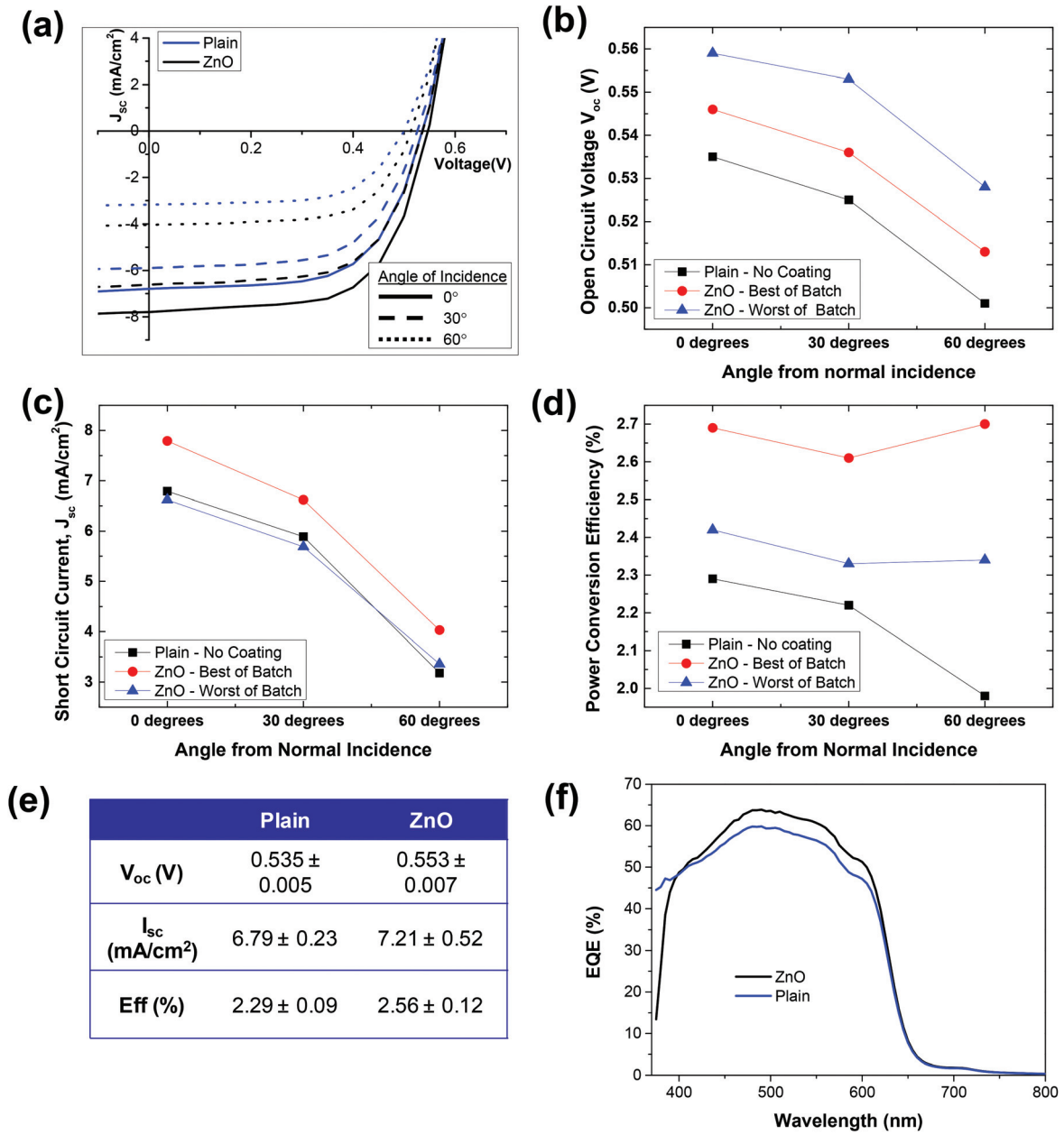

	Plain	ZnO
V_{oc} (V)	0.535 ± 0.005	0.553 ± 0.007
I_{sc} (mA/cm^2)	6.79 ± 0.23	7.21 ± 0.52
Eff (%)	2.29 ± 0.09	2.56 ± 0.12

Fig. 3 (a) *J*–*V* characteristics of NW solar cells, (b) open circuit voltage, (c) short circuit currents and (d) efficiencies of the cells at various incidence angles of light. Note the efficiencies are corrected for light intensity change with tilt, (e) table showing average values and standard deviation for the samples measured and (f) comparison of the external quantum efficiency (EQE) of representative samples.

ZnO NWs (450 nm) on ITO glass is shown in Fig. 4(a). Due to the large bandgap of ZnO (3.2 eV), and the ordered nature of the array, highly crystalline ZnO NWs show high and constant transmittance in the visible range and good absorbance in the UV. A sharp drop can be observed below 400 nm. The consequent reduction of UV reaching the active polymer layer is expected to increase the lifetime of the solar cell. In order to quantify this effect, several OPV cells were tested under accelerated conditions. For this, they were not sealed (allowing air access) and shone continuously with a UV lamp (peaks at 254 nm, 313 nm and 365 nm) 10 cm away. At regular time intervals, the IV curves of the cells were measured under AM 1.5 conditions. The V_{oc} remained constant during the UV exposure. The normalised I_{sc} change with time is shown in Fig. 4(b), showing a reduced decay rate in the presence of ZnO NWs.

Self cleaning

Under practical conditions, mounted photovoltaic arrays eventually become covered with a fine layer of dirt and dust, decreasing the amount of light reaching the cells. The amount of power loss due to soiling depends on variables such as

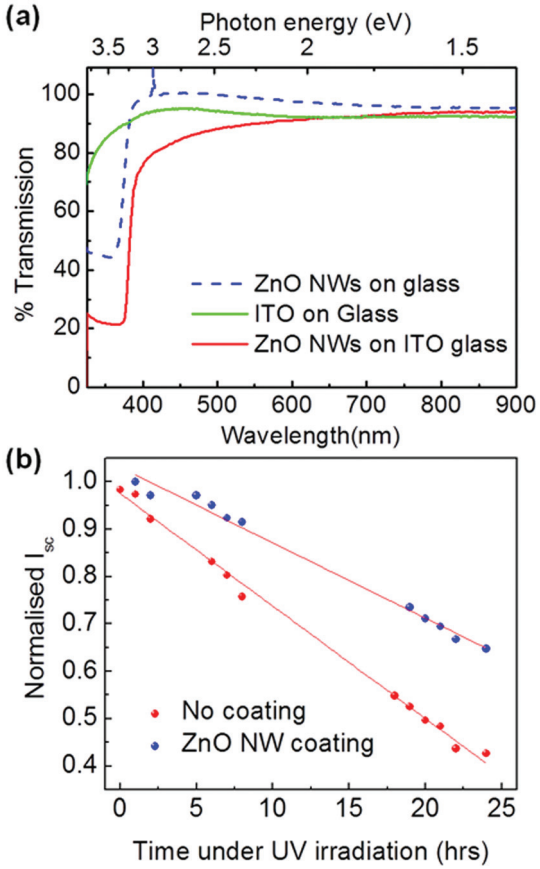

Fig. 4 (a) Transmission spectra of bare ITO glass, and 450 nm ZnO NWs on bare and ITO coated glass measured with a Thermoelectron UV-VIS spectrometer and (b) normalised short circuit current of P3HT–PCBM cells degraded by exposing constantly to a high intensity UV lamp.

location, the type of dust, and the weather pattern. Decreases in efficiency due to soiling from 0.03 to 0.3% per day[26,33] have been reported. The same ZnO NW coating may also be used to provide self-cleaning properties to the solar panels, and two distinct routes can be used to achieve this effect.

For regions where organic soiling is predominant, the photocatalytic nature of ZnO can be exploited. Photocatalytic stain photo-decomposition was tested by measuring the degradation rate of methylene blue (MB) dye. The absorption spectrum of MB in a water solution was measured in a quartz cuvette, using a water filled cuvette as a reference. Three 1.5 cm^2 glass electrodes were prepared, one plain glass, another coated with a sputtered ZnO thin film and finally one with ZnO NWs, each placed in different MB containing cuvettes and placed under UV light. The absorption spectra of the solution were measured every hour. The intensity of the MB absorption peak as a function of time and the colour of the solution before and after degradation are shown in Fig. 5. Some degradation occurs in the presence of UV even using bare glass. The presence of a ZnO thin film increases this rate and the NWs, due to their higher surface area, breakdown the dye at the highest rate.

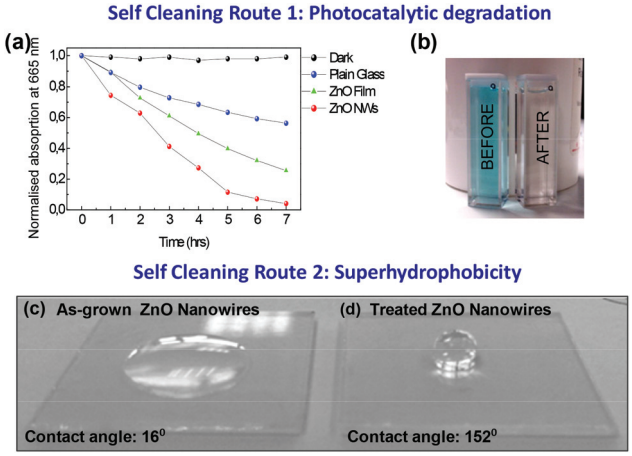

Fig. 5 (a) Rate of photo-decomposition of MB dye in water by ZnO NWs on glass (as measured by the size of the main absorption peak). ZnO thin film, plain glass and dark measurements are also provided for comparison. (b) Photograph showing the decolouration of the dye after breakdown under the presence of ZnO, (c) water droplet on an as grown ZnO NW array (superhydrophilic) and (d) on a stearic acid treated array (superhydrophobic).

The as-grown NWs are highly hydrophilic. Oxide thin films are industrially in use for antifogging since water spreads and forms a sheet across the surface instead of forming innumerable tiny droplets. An alternative route to self-cleaning is known as the Lotus effect. A combination of hydrophobic materials and air-filled porous surface structure (Cassie-Baxter effect) results in a superhydrophobic surface. This results in large contact angles of water on the surface, allowing it to roll off at minimum surface tilt, carrying dust particles with it, as it is more energetically favourable to conform to the particle than to air or the surface.

Xu *et al.* reported the fabrication of simultaneous superhydrophobic and antireflective coatings from silica nanoparticle sol–gel methods.[34] The silica particles were modified with a layer of hexamethyldisilazane, to obtain their superhydrophobicity. Our ZnO NWs have the required porous texture, but not the right surface energy. Treating them with a layer of a hydrophobic molecule (*e.g.* stearic acid, 1 mM overnight)[27] dramatically changes the surface behaviour from highly hydrophilic to superhydrophobic (Fig. 5(c and d)), opening an alternative route for a self-cleaning surface, more suitable for dusty environments with some rainfall.

Conclusions

ZnO NW arrays are demonstrated as multifunctional antireflection coatings, and applied to OPVs for the first time. ZnO NWs on OPV cells increased optical absorption and resulted in an increase (up to 36%) in efficiency of the devices compared to their plain counterparts. The enhancement of efficiency was strongest at high tilt angles. UV absorption through the NWs

improved cell lifetime, reduced the degradation rate by ~50% under accelerated lifetime testing conditions. Finally, the NW coating was demonstrated to be selectively tuned to show both aspects of self-cleaning behaviour, the superhydrophobic lotus effect and photocatalytic degradation. Our results revealed the potential of ZnO NWs to be used as transparent, self-cleaning coatings which could potentially be applied in architecture or automobile windows, eyeglasses, optical windows for electronic devices, *etc*.

Acknowledgements

PH and GA would like to acknowledge the support from the Nokia – Cambridge University Strategic Research Alliance in Nanoscience and Nanotechnology. HEU acknowledges support from the Distinguished Young Scientist Award of the Turkish Academy of Sciences (TUBA). H. Zhou acknowledges support from NSFC (No. 61204077). WA would like to thank National Research Council, Sri Lanka. HB would like to thank the Leverhulme Trust for the research grant. The authors acknowledge Bin Li and Xiao Du for their assistance in measuring optical properties in an integrating sphere.

Notes and references

1 *Retail Price Summary*. (NPD Solar Buzz). at <http://www.solarbuzz.com/facts-and-figures/retail-price-environment/module-prices>.
2 Z. He, *et al.*, Enhanced power-conversion efficiency in polymer solar cells using an inverted device structure, *Nat. Photonics*, 2012, **6**, 591–595.
3 J.-J. Simon, *et al.*, Electromagnetic field optimization for enhancing photovoltaic efficiency of organic solar cells. in *Opt. Interf. Coatings* FB3 (Optical Society of America, 2004). at <http://www.opticsinfobase.org/abstract.cfm?URI=OIC-2004-FB3>.
4 C. Eisele, C. E. Nebel and M. Stutzmann, Periodic light coupler gratings in amorphous thin film solar cells, *J. Appl. Phys.*, 2001, **89**, 7722–7726.
5 W.-E. Hsu, C.-T. Lee and H. Y. Lin, Luminous-efficiency improvement of solar-cell-integrated high-contrast organic light-emitting diode by applying distributed Bragg reflector, *J. Soc. Inf. Disp.*, 2011, **19**, 847–853.
6 L. Zeng, *et al.*, Efficiency enhancement in Si solar cells by textured photonic crystal back reflector, *Appl. Phys. Lett.*, 2006, **89**, 111111.
7 S. Pillai, K. R. Catchpole, T. Trupke and M. A. Green, Surface plasmon enhanced silicon solar cells, *J. Appl. Phys.*, 2007, **101**, 093105.
8 S.-S. Kim, S.-I. Na, J. Jo, D.-Y. Kim and Y.-C. Nah, Plasmon enhanced performance of organic solar cells using electrodeposited Ag nanoparticles, *Appl. Phys. Lett.*, 2008, **93**, 073307.
9 E. Stratakis and E. Kymakis, Nanoparticle-based plasmonic organic photovoltaic devices, *Mater. Today*, 2013, **16**, 133–146.
10 D. Duché, *et al.*, Slow Bloch modes for enhancing the absorption of light in thin films for photovoltaic cells, *Appl. Phys. Lett.*, 2008, **92**, 193310.
11 W.-L. Min, B. Jiang and P. Jiang, Bioinspired Self-Cleaning Antireflection Coatings, *Adv. Mater.*, 2008, **20**, 3914–3918.
12 L. Hu and G. Chen, Analysis of optical absorption in silicon nanowire arrays for photovoltaic applications, *Nano Lett.*, 2007, **7**, 3249–3252.
13 K. Peng, *et al.*, Aligned single-crystalline Si nanowire arrays for photovoltaic applications, *Small*, 2005, **1**, 1062–1067.
14 O. L. Muskens, J. G. Rivas, R. E. Algra, E. P. a M. Bakkers and A. Lagendijk, Design of light scattering in nanowire materials for photovoltaic applications, *Nano Lett.*, 2008, **8**, 2638–2642.
15 Y.-C. Chao, C.-Y. Chen, C.-A. Lin and J.-H. He, Light scattering by nanostructured anti-reflection coatings, *Energy Environ. Sci.*, 2011, **4**, 3436–3441.
16 Y.-A. Dai, *et al.*, Subwavelength Si nanowire arrays for self-cleaning antireflection coatings, *J. Mater. Chem.*, 2010, **20**, 10924.
17 Y. Lee, D. S. Ruby, D. W. Peters, B. B. Mckenzie and J. W. P. Hsu, ZnO Nanostructures as Efficient Antireflection Layers in Solar Cells, *Nano Lett.*, 2008, **8**, 1501–1505.
18 H. Takato, *et al.*, Effects of Optical Confinement in Textured Antireflection Coating using ZnO Films for Solar Cells, *Jpn. J. Appl. Phys.*, 1992, **31**, L1665–L1667.
19 L. Vayssieres, Growth of Arrayed Nanorods and Nanowires of ZnO from Aqueous Solutions, *Adv. Mater.*, 2003, **15**, 464–466.
20 H. E. Unalan, *et al.*, Rapid synthesis of aligned zinc oxide nanowires, *Nanotechnology*, 2008, **19**, 255608.
21 Y.-J. Lee, D. S. Ruby, D. W. Peters, B. B. McKenzie and J. W. P. Hsu, ZnO Nanostructures as Efficient Antireflection Layers in Solar Cells, *Nano Lett.*, 2008, **8**, 1501–1505.
22 P. Aurang, O. Demircioglu, F. Es, R. Turan and H. E. Unalan, ZnO Nanorods as Antireflective Coatings for Industrial-Scale Single-Crystalline Silicon Solar Cells, *J. Am. Ceram. Soc.*, 2013, **96**, 1253–1257.
23 J. Y. Chen and K. W. Sun, Growth of vertically aligned ZnO nanorod arrays as antireflection layer on silicon solar cells, *Sol. Energy Mater. Sol. Cells*, 2010, **94**, 930–934.
24 A. Rivaton, *et al.*, Light-induced degradation of the active layer of polymer-based solar cells, *Polym. Degrad. Stab.*, 2010, **95**, 278–284.
25 S. Chakrabarti and B. K. Dutta, Photocatalytic degradation of model textile dyes in wastewater using ZnO as semiconductor catalyst, *J. Hazard. Mater.*, 2004, **112**, 269–278.
26 J. R. Caron and B. Littmann, Direct Monitoring of Energy Lost Due to Soiling on First Solar Modules in California, *IEEE J. Photovoltaics*, 2013, **3**, 336–340.
27 C. Badre, T. Pauporté, M. Turmine and D. Lincot, A ZnO nanowire array film with stable highly water-repellent properties, *Nanotechnology*, 2007, **18**, 365705.

28 X. Zhang, F. Shi, J. Niu, Y. Jiang and Z. Wang, Superhydrophobic surfaces: from structural control to functional application, *J. Mater. Chem.*, 2008, **18**, 621.
29 L. E. Greene, *et al.*, Low-Temperature Wafer-Scale Production of ZnO Nanowire Arrays, *Angew. Chem., Int. Ed.*, 2003, **42**, 3031–3034.
30 X. He, *et al.*, Formation of Well-Ordered Heterojunctions in Polymer:PCBM Photovoltaic Devices, *Adv. Funct. Mater.*, 2011, **21**, 139–146.
31 L. J. A. Koster, V. D. Mihailetchi, R. Ramaker and P. W. M. Blom, Light intensity dependence of open-circuit voltage of polymer:fullerene solar cells, *Appl. Phys. Lett.*, 2005, **86**, 123509.
32 J. Y. Kim, *et al.*, New Architecture for High-Efficiency Polymer Photovoltaic Cells Using Solution-Based Titanium Oxide as an Optical Spacer, *Adv. Mater.*, 2006, **18**, 572–576.
33 A. Kimber, L. Mitchell, S. Nogradi and H. Wenger, The Effect of Soiling on Large Grid-Connected Photovoltaic Systems in California and the Southwest Region of the United States, in *Conf. Rec. 2006 IEEE 4th World Conf. Photovolt. Energy Convers.*, 2006, vol. **2**, pp. 2391–2395.
34 L. Xu, L. Gao and J. He, Fabrication of visible/near-IR antireflective and superhydrophobic coatings from hydrophobically modified hollow silica nanoparticles and poly(methyl methacrylate), *RSC Adv.*, 2012, **2**, 12764–12769.

